PHILOSOPHICAL TRANSACTIONS OF THE ROYAL SOCIETY A MATHEMATICAL, PHYSICAL & ENGINEERING SCIENCES

Wave Intensity Analysis of High Frequency Vibrations

Robin S. Langley and Ahmet N. Bercin

Phil. Trans. R. Soc. Lond. A 1994 **346**, 489-499
doi: 10.1098/rsta.1994.0031

Wave intensity analysis of high frequency vibrations

By Robin S. Langley[1] and Ahmet N. Bercin[2]

[1] *Department of Aeronautics and Astronautics, University of Southampton, Southampton SO9 5NH, U.K.*

[2] *College of Aeronautics, Cranfield Institute of Technology, Cranfield, Bedford MD43 0AL, U.K.*

In the statistical energy analysis (SEA) approach to high frequency dynamics it is assumed that the vibrational wavefield in each component of an engineering structure is diffuse. In some instances the directional filtering effects of structural joints can lead to highly non-diffuse wavefields, and in such cases SEA will yield a very poor estimate of the vibrational response. An alternative approach is presented here in which the directional dependency of the vibrational wavefield in each component is modelled by using a Fourier series. It is shown that, if required, the resulting energy balance equations may be cast in the form of conventional SEA with the addition of 'non-direct' coupling loss factors. The method is applied to the bending and in-plane vibrations of various plate structures and a comparison is made with exact results yielded by the dynamic stiffness method. A significant improvement over conventional SEA is demonstrated.

1. Introduction

The analysis of high-frequency vibration levels in engineering structures causes severe difficulties for standard analysis procedures such as the finite element method (Zienkiewicz 1977). This approach, and all others that are based on the solution of the governing constitutive equations, requires an excessive number of degrees of freedom to capture the short wavelength structure deformation that occurs at high frequencies. A well-known alternative approach is statistical energy analysis (SEA) (Lyon 1975) in which a complex structure is represented as an assembly of subsystems whose vibrational energy levels are calculated from power balance considerations.

A central tenet of SEA is that within a subsystem there is 'equipartition' of vibrational energy among the constituent modes. From a wave, rather than a modal, point of view, this principle is equivalent to assuming that the vibrational wavefield in each structural element is diffuse. Although this assumption may be reasonable in many cases, there are instances where the directional filtering effect of structural junctions can lead to wavefields that are far from diffuse; in such cases SEA yields a very poor estimate of the vibrational energy levels (Blakemore *et al.* 1990; Langley 1992). In this paper an alternative approach is presented in which the directional dependence of the vibrational wave intensity in each structural component is modelled by using a Fourier series; if a single Fourier term is used, then conventional

Phil. Trans. R. Soc. Lond. A (1994) **346**, 489–499
Printed in Great Britain

SEA is recovered. This approach, which is referred to as wave intensity analysis (WIA), was first developed by Langley (1992) who demonstrated that the method can yield much improved estimates for the bending vibrations of plate structures.

It is shown here that the power balance equations that arise in WIA may, if required, be cast in the form of conventional SEA with the addition of 'non-direct' coupling loss factors between subsystems which are not physically connected. This is consistent with the analysis of Langley (1989*b*, 1990) who demonstrated that non-direct coupling loss factors may be of significant effect even for structures which satisfy the conditions which are normally laid down for the successful application of conventional SEA. The method is applied here to a range of plate structures, and a comparison is made with exact calculations based on the dynamic stiffness method. Whereas Langley (1992) considered only bending vibrations, both bending and in-plane vibrations are considered here, and a significant improvement over conventional SEA is demonstrated.

2. Wave intensity analysis

Engineering structures are normally composed of a number of regular structural elements such as beams, plates, and shells, which are either bolted, welded, or bonded together. The differential equation which governs the dynamic response of a typical element may be written in the general form

$$\boldsymbol{L}(\boldsymbol{w})-\rho\,\partial^2\boldsymbol{w}/\partial t^2=\boldsymbol{F}(\boldsymbol{x},t), \tag{2.1}$$

where $\boldsymbol{w}(\boldsymbol{x},t)$ is the displacement vector at the spatial location $\boldsymbol{x}$, ρ is the mass density, and $\boldsymbol{F}(\boldsymbol{x},t)$ is the applied distributed loading. Further $\boldsymbol{L}$ is a structural differential operator which characterizes the component: in what follows it will be assumed that each component is homogeneous, so that $\boldsymbol{L}$ does not vary with spatial position. Equation (2.1) can be used to determine the various types of elastic wave which can be borne by the component. The concern here is with harmonic plane waves which have the form $\boldsymbol{w}=\boldsymbol{a}\exp(\mathrm{i}\boldsymbol{k}.\boldsymbol{x}-\mathrm{i}\omega t)$, where $\boldsymbol{k}$ is the wavenumber vector, ω is the circular frequency, and $\boldsymbol{a}$ is the wave 'mode'. Valid solutions for $\boldsymbol{k}$ and $\boldsymbol{a}$ at a specified frequency ω may be sought by substituting the assumed wave form into the homogeneous version of equation (2.1). This yields

$$[\boldsymbol{\Lambda}(\boldsymbol{k})-\rho\omega^2\boldsymbol{I}]\,\boldsymbol{a}=\boldsymbol{0}, \tag{2.2}$$

where $\boldsymbol{I}$ is the identity matrix and the detailed form of the matrix $\boldsymbol{\Lambda}$ is determined by the operator $\boldsymbol{L}$. The n-dimensional wavenumber vector $\boldsymbol{k}$ may be expressed in terms of the scalar wavenumber $\mu=|\boldsymbol{k}|$ and a set of $n-1$ direction cosines, $\boldsymbol{\theta}$ say. With this notation equation (2.2) takes the form

$$[\boldsymbol{\Lambda}(\mu,\boldsymbol{\theta})-\rho\omega^2\boldsymbol{I}]\,\boldsymbol{a}=\boldsymbol{0}. \tag{2.3}$$

For specified ω and $\boldsymbol{\theta}$, this is an eigenproblem that may be solved to yield the set of eigenvalues μ_j and eigenvectors $\boldsymbol{a}_j$. The number of distinct real values of μ thus obtained is equal to the number of distinct types of propagating plane wave of heading $\boldsymbol{\theta}$ that can be borne by the element. For an isotropic element equation (2.3) is independent of $\boldsymbol{\theta}$ and the various wavetypes may propagate in all directions. An example in this category is a flat plate element that will display three distinct values of μ, corresponding to out-of-plane bending waves, in-plane shear waves, and in-plane longitudinal waves.

PHILOSOPHICAL TRANSACTIONS OF THE ROYAL SOCIETY A MATHEMATICAL, PHYSICAL & ENGINEERING SCIENCES

In what follows the high-frequency vibrational response of an engineering structure is described purely in terms of elastic waves. It is assumed that the harmonic response of a typical element may be written in the form

$$\boldsymbol{w}(\boldsymbol{x},t) = \sum_j \int_\theta f_j(\boldsymbol{\theta})\, \boldsymbol{a}_j(\boldsymbol{\theta}) \exp\left[i\boldsymbol{k}(\mu_j,\boldsymbol{\theta}).\boldsymbol{x} - \mathrm{i}\omega t\right] \mathrm{d}\boldsymbol{\theta}, \tag{2.4}$$

where the sum is over the number of distinct wavetypes displayed by the element and the integral is over the range of possible wave headings; function $f_j(\boldsymbol{\theta})$ represents the amplitude of wavetype j at heading $\boldsymbol{\theta}$. It is further assumed that all phase effects may be neglected, which implies that the various wave components may be considered to be uncorrelated. This assumption has two consequences: first, the response in each component as given by equation (2.4) will be homogeneous with respect to the location $\boldsymbol{x}$, and second, resonance peaks and anti-resonance troughs which are caused by phase effects will not arise. There is evidence to suggest that at high frequencies the response does tend to become homogeneous providing that the element is reverberant, has a high modal overlap factor, and a high number of modes are excited: this aspect has been studied both theoretically and experimentally by Dowell & Kubota (1985, 1986). Further, at high modal overlap the resonant peaks do not differ greatly from the frequency average response level, which implies that phase effects are not significant; at low modal overlap the present approach can be expected to yield a result which corresponds to the average response over a frequency band which contains a number of resonant peaks. If the assumption of uncorrelated wave components is adopted, then equation (2.4) implies that the vibrational energy density within a typical element may be written in the form

$$e(\omega) = \sum_j \int_\theta e_j(\boldsymbol{\theta},\omega)\, \mathrm{d}\boldsymbol{\theta}, \tag{2.5}$$

where $e_j(\boldsymbol{\theta},\omega)$ is the energy density associated with wavetype j at heading $\boldsymbol{\theta}$. The quantities $e_j(\boldsymbol{\theta},\omega)$ are taken to be the basic unknowns in the present analysis method, and a solution is sought by considering power balance.

Although $e_j(\boldsymbol{\theta},\omega)$ has previously been used to represent the energy density of the jth wavetype in a particular component, the notation may be extended so that j is considered to range over all wavetypes in all components of the built up structure. Thus, for example, in the case of a structure consisting of two coupled plates j would range from 1 to 6, covering the three wavetypes which occur in each plate. For each wavetype j the power input through external forcing, P_j^{in} say, together with the power input over the element boundaries P_j^{ci}, must be balanced by the dissipated power P_j^{diss} and the power output over the element boundaries P_j^{co}. Thus

$$P_j^{\mathrm{in}}(\boldsymbol{\theta},\omega) = P_j^{\mathrm{diss}}(\boldsymbol{\theta},\omega) + P_j^{\mathrm{co}}(\boldsymbol{\theta},\omega) - P_j^{\mathrm{ci}}(\boldsymbol{\theta},\omega). \tag{2.6}$$

Now most theoretical models of damping imply that the dissipated power is proportional to the mean stored energy, so that

$$P_j^{\mathrm{diss}}(\boldsymbol{\theta},\omega) = \omega\eta_j A_j\, e_j(\boldsymbol{\theta},w) = \omega\eta_j E_j(\boldsymbol{\theta},\omega), \tag{2.7}$$

where η_j is the loss factor, A_j is the length, area, or volume of the relevant structural element, and $E_j = A_j e_j$ is the total energy stored in wavetype j at heading $\boldsymbol{\theta}$. The power output by wavetype j at a boundary of the element may be written in the form

$$P_j^{\mathrm{co}}(\boldsymbol{\theta},\omega) = e_j(\boldsymbol{\theta},\omega)\, c_{gj}(\boldsymbol{\theta},\omega) \cos(\delta)\, L, \tag{2.8}$$

where c_{gj} is the group velocity of the wave, δ is the angle between the wave heading and the outward pointing normal to the boundary (assumed to be constant over the boundary), and L is the appropriate dimension (unity, length or area) of the boundary. As the concern is with power output, equation (2.8) relates only to those wave headings for which $0 \leqslant \delta \leqslant \frac{1}{2}\pi$. For clarity, the present analysis is now limited to two-dimensional isotropic components, although in general the method is equally applicable to the full range of structural types. It is also convenient at this stage to introduce the modal density ν_j which is associated with wavetype j for a two-dimensional isotropic element: $\nu_j = \omega A_j/2\pi c_j c_{gj}$, where c_j is the wave phase velocity and A_j is the area of the element. Equation (2.8) can now be written in the form

$$P_j^{\mathrm{co}}(\theta,\omega) = (\omega L/2\pi)[E_j(\theta,\omega)/\nu_j][\cos(\theta+\tfrac{1}{2}\pi-\psi)/c_j], \tag{2.9}$$

where the angle ψ is used to describe the orientation of the boundary, as shown in figure 1*a*.

It can be noted that in two dimensions the direction cosine vector $\boldsymbol{\theta}$ reduces to the scalar wave heading θ. Equation (2.9) relates to a single output boundary: more generally the result must be summed over all boundaries of the element for which $0 \leqslant \delta \leqslant \frac{1}{2}\pi$.

The final term which appears in equation (2.6) is the power input to heading θ of wavetype j at the element boundaries. This power will be supplied by one or more of the other wavetypes; for example, figure 1*b* illustrates the case in which the power is supplied by heading ϕ of wavetype i. The power input to a band $\mathrm{d}\theta$ of wavetype j may in this case be written in the form

$$P_j^{\mathrm{ci}}(\theta,\omega)\,\mathrm{d}\theta = e_i(\phi,\omega)\,c_{gi}(\omega)\cos(\phi+\tfrac{1}{2}\pi-\psi)\,L\tau_{ij}(\phi+\tfrac{1}{2}\pi-\psi)\,\mathrm{d}\phi, \tag{2.10}$$

where τ_{ij} is the transmission coefficient between the two wavetypes. By making use of Snell's Law and introducing the modal density of wavetype i, equation (2.10) may be rewritten as

$$P_j^{\mathrm{ci}}(\theta,\omega) = (\omega L/2\pi)[E_i(\phi,\omega)/\nu_i][\cos(\theta+\tfrac{1}{2}\pi-\psi)/c_j]\,\tau_{ij}(\phi+\tfrac{1}{2}\pi-\psi). \tag{2.11}$$

This result relates to a single input wavetype and a single input boundary; more generally the total power input may be obtained by summing over the relevant boundaries and wavetypes.

By combining equations (2.6), (2.7), (2.9) and (2.11), the total power balance equation for heading θ of wavetype j may be written in the form

$$P_j^{\mathrm{in}}(\theta,\omega) = \omega\eta_j E_j(\theta,\omega) + (\omega/2\pi c_j)[E_j(\theta,\omega)/\nu_j]\sum_k L_k\cos(\theta+\tfrac{1}{2}\pi-\psi_k)$$

$$-(\omega/2\pi c_j)\sum_m\sum_i[E_i(\phi_{mi},\omega)/\nu_i]L_m\cos(\theta+\tfrac{1}{2}\pi-\psi_m)\,\tau_{ij}^m(\phi_{mi}+\tfrac{1}{2}\pi-\psi_m), \tag{2.12}$$

where the sum over k represents the output boundaries and the sums over m and i correspond to the input boundaries and the input wavetypes. An equation of this form may be derived for each wavetype j and in principle the set of coupled equations can then be solved to yield the wave energies $E_j(\theta,\omega)$. A convenient approach to the solution of these equations is to expand the angular dependency of the wave energies in the form of a Fourier series so that

$$E_j(\theta,\omega) = \sum_p E_{jp}(\omega)N_p(\theta), \tag{2.13}$$

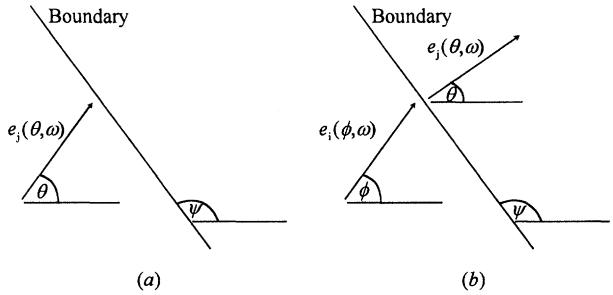

(*a*) (*b*)

Figure 1. Schematic of wave incidence at a boundary.

where the shape functions $N_p(\theta)$ represent the $\cos(m\theta)$ and $\sin(m\theta)$ Fourier terms. By substituting (2.13) into (2.12) and using the Galerkin procedure, the following set of linear equations may be derived

$$\boldsymbol{C}\hat{\boldsymbol{E}} = \boldsymbol{P}. \tag{2.14}$$

Here the vector $\hat{\boldsymbol{E}}$ contains the coefficients E_{jp}/ν_j and the entries of the matrix $\boldsymbol{C}$ and the $\boldsymbol{P}$ are given by

$$C_{jp,is} = \delta_{ij}\left\{\omega\eta_j\nu_j\int_0^{2\pi} N_p(\theta)N_s(\theta)\,\mathrm{d}\theta + (\omega/2\pi c_j)\sum_k L_k\int_{\theta_k} N_p(\theta)N_s(\theta)\cos(\theta+\tfrac{1}{2}\pi-\psi_k)\,\mathrm{d}\theta\right\}$$

$$-(\omega/2\pi c_j)\sum_m L_m\int_{\theta_m} N_p(\theta)N_s(\phi_{mi})\cos(\theta+\tfrac{1}{2}\pi-\psi_m)\,\tau_{ij}^m(\phi_{mi}+\tfrac{1}{2}\pi-\psi_m)\,\mathrm{d}\theta, \tag{2.15}$$

$$P_{jp} = \int_0^{2\pi} P_j^{\mathrm{in}}(\theta,\omega)N_p(\theta)\,\mathrm{d}\theta. \tag{2.16}$$

As presented above, the matrix $\boldsymbol{C}$ is not symmetric. The Fourier shape functions can be grouped into those for which $N(\theta) = N(\theta+\pi)$ (type A, say) and those for which $N(\theta) = -N(\theta+\pi)$ (type B, say); it can be shown that coupling terms involving two type A or two type B Fourier components are symmetric, while those involving a type A and a type B Fourier component are skew-symmetric. The matrix may readily be made symmetric by multiplying those rows corresponding to type B Fourier components by -1. In what follows it will be assumed that this has been done; the resulting symmetry of the matrix has important implications, as discussed in §3*b*. The relation between the present approach and conventional SEA is discussed in the following section.

3. Relation to statistical energy analysis

(*a*) *Conventional SEA*

The simplest approximation to the angular dependence of the wave energies $E_j(\theta,\omega)$ is to assume that each wave field is diffuse, so that $E_j(\theta,\omega) = E_{j1}(\omega)/2\pi$, which corresponds to the use of a single Fourier term in equation (2.13). If both sides of equation (2.14) are in this case multiplied by 2π then it has been shown by Langley (1992) that a typical coupling term in the matrix $\boldsymbol{C}$ will take the form

$$C_{j1,i1} = -\omega\nu_j\sum_m \eta_{ji}^m, \quad \eta_{ji}^m = L_m\, c_{\mathrm{g}j}\langle\tau_{ji}^m\rangle/(\omega A_j\,\pi). \tag{3.1, 3.2}$$

Here η_{ij}^m is the coupling loss factor as used in SEA, and $\langle \tau_{ij}^m \rangle$ is the diffuse wave field transmission coefficient (Lyon 1975). Similarly, Langley (1992) has shown that a diagonal term in the matrix $\boldsymbol{C}$ will take the form

$$C_{j1,j1} = \omega \eta_j \nu_j + \omega \nu_j \sum_m \sum_{i \neq j} \eta_{ji}^m. \tag{3.3}$$

Equations (3.1) and (3.3), together with equation (2.14) constitute conventional SEA. It thus follows that the present method reduces to standard SEA if a single Fourier component is used in equation (2.13): in this regard the present approach may be considered to be a natural generalization of SEA.

(*b*) *SEA with non-direct coupling loss factors*

It has been suggested that in some applications SEA should include coupling loss factors between subsystems which are not directly coupled (for example, Blakemore *et al.* 1990). In fact Langley (1990) has demonstrated that in general these coupling loss factors are non-zero, and further there is no sound theoretical reason for assuming that they are negligibly small. However, the calculation of these terms presents severe difficulties and a general methodology has yet to appear in the literature. It is shown in this section that WIA provides just such a methodology: equations (2.14)–(2.16) may be recast in the form of conventional SEA with the addition of non-direct coupling loss factors.

The energy vector $\hat{\boldsymbol{E}}$ which appears in equation (2.14) may be partitioned in the form $\hat{\boldsymbol{E}} = (\hat{\boldsymbol{E}}_1 : \hat{\boldsymbol{E}}_n)$ where $\hat{\boldsymbol{E}}_1$ contains the diffuse energy components: i.e. those components which are related to the first (constant) term in the Fourier expansion of the angular distribution of the wave energy. The partition $\hat{\boldsymbol{E}}_n$ contains the energy terms which are associated with the second and subsequent terms in the Fourier expansion. Two points regarding $\hat{\boldsymbol{E}}_1$ can be noted: first, the terms $\hat{\boldsymbol{E}}_1$ are exactly the energy variables which appear in SEA and second, knowledge of $\hat{\boldsymbol{E}}_1$ alone is sufficient to yield the total energy in an element, as the integral over θ of all but the first Fourier term is zero. The central WIA equation, equation (2.14), may be partitioned in terms of $\hat{\boldsymbol{E}}_1$ and $\hat{\boldsymbol{E}}_n$ to yield

$$\begin{pmatrix} \boldsymbol{C}_{11} & \boldsymbol{C}_{1n} \\ \boldsymbol{C}_{1n}^{\mathrm{T}} & \boldsymbol{C}_{nn} \end{pmatrix} \begin{pmatrix} \hat{\boldsymbol{E}}_1 \\ \hat{\boldsymbol{E}}_n \end{pmatrix} = \begin{pmatrix} \boldsymbol{P}_1 \\ \boldsymbol{P}_n \end{pmatrix}. \tag{3.4}$$

The symmetry of $\boldsymbol{C}$, as noted in §2, has been employed in this equation. Given the definition of $\hat{\boldsymbol{E}}_1$ it follows that $\boldsymbol{C}_{11}$ is precisely the matrix which appears in conventional SEA. Equation (3.4) can be recast in the form

$$(\boldsymbol{C}_{11} - \boldsymbol{C}_{1n}\, \boldsymbol{C}_{nn}^{-1}\, \boldsymbol{C}_{1n}^{\mathrm{T}})\, \hat{\boldsymbol{E}}_1 = \boldsymbol{P}_1 - \boldsymbol{C}_{1n}\, \boldsymbol{C}_{nn}\, \boldsymbol{P}_n. \tag{3.5}$$

The result is essentially SEA with the addition of the triple matrix product which appears on the left-hand side: this symmetric matrix will contain non-direct coupling loss factors. The additional power term which appears on the right-hand side will generally be small or zero, since for most types of loading the input power tends to be fairly diffuse, so that $\boldsymbol{P}_n \approx 0$. Three important conclusions follow from equation (3.5): (i) the non-direct coupling loss factors are independent of the applied loading, (ii) the non-direct coupling loss factors are dependent on the system loss factors, as the diagonals of $\boldsymbol{C}_{nn}$ involve these terms, and (iii) the present approach provides a reasonably straightforward method by which the non-direct coupling loss factors may be calculated.

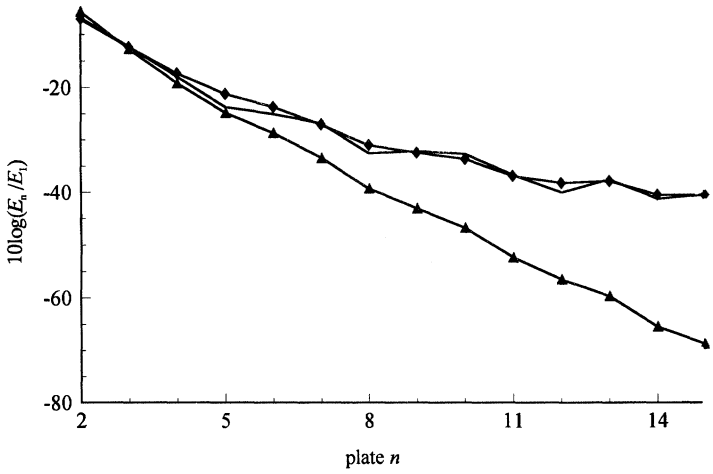

Figure 2. Bending energy distribution in the fifteen plate structure for the one-third octave band with centre frequency 5 kHz. Unmarked curve: exact results. Diamond symbols: WIA results. Triangle symbols: SEA results.

4. Example applications

In this section the foregoing theory is applied to two example structures. The first consists of a chain of 15 plates which are all of width 0.85 m. Each plate is rigidly attached at 90° to its neighbours in the chain so that every second plate is vertical while the remaining plates are horizontal. The structure is taken to be simply supported along the two longitudinal edges and clamped along the two transverse edges. The lengths of the plates (in metres) are 0.9, 1.37, 1.45, 1.1, 0.7, 1.1, 0.9, 0.55, 0.75, 1.1, 0.7, 0.65, 0.95, 0.78 and 1.15. The thicknesses of the plates (in millimetres) are 10, 6.5 8.4, 3.6, 4.5, 6.3, 5.5, 3.0, 4.4, 5.6, 6.0, 4.0, 3.5, 5.2 and 6.5. Each plate is made from steel, which has Young's modulus $E = 2 \times 10^{11}$ N m^{-2}, mass density $\rho =$ 7800 kg m^{-3}, and Poisson ratio $\nu = 0.3$. Exact results for the dynamic response of this structure have been obtained by using the direct dynamic stiffness method. The formulation used represents an extension of the work of Langley (1989*a*) to the case of in-plane vibrations: full details are given by Bercin (1993). The response of the structure to an out-of-plane harmonic point load applied to the first plate has been computed over the frequency range 0.5–20 kHz, and the results obtained have been averaged over nine randomly selected point load locations in the first plate. The average vibrational energy of each plate thus obtained has then been further averaged over sixteen one-third octave bands to yield a frequency response curve which may be compared with SEA and WIA. The modal densities and group velocities that are required by SEA and WIA are standard for plate structures (see, for example, Cremer *et al.* 1988), while the junction wave transmission coefficients have been calculated by using the method of Langley & Heron (1990). Because of symmetry only cosine Fourier terms were used in the WIA technique, and five terms were used for the inner plates while three terms were used for the two outmost plates.

Results for the bending vibrational energy of each plate for the one-third octave band with centre frequency 5 kHz are shown in figure 2. It is clear that the WIA approach yields a very good estimate of the response, whereas SEA tends to overestimate the response for plate 2 and severely underestimate the response for subsequent plates. This is because the wave filtering effect of the structural junctions

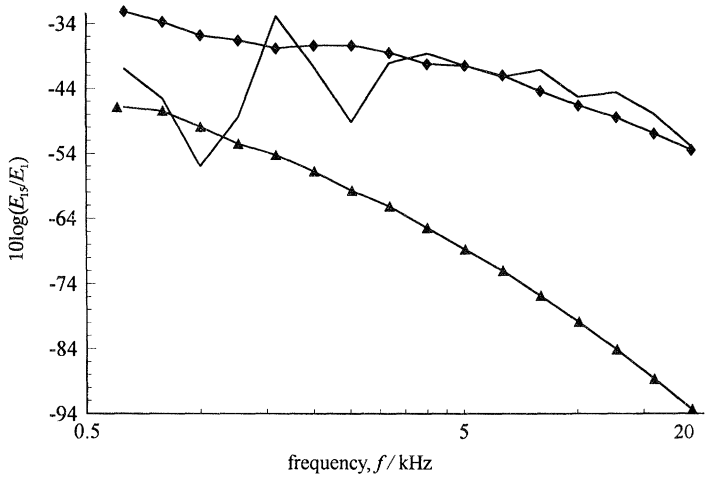

Figure 3. Bending energy in the last plate of the fifteen plate structure. Unmarked curve: exact results. Diamond symbols: WIA results. Triangle symbols: SEA results.

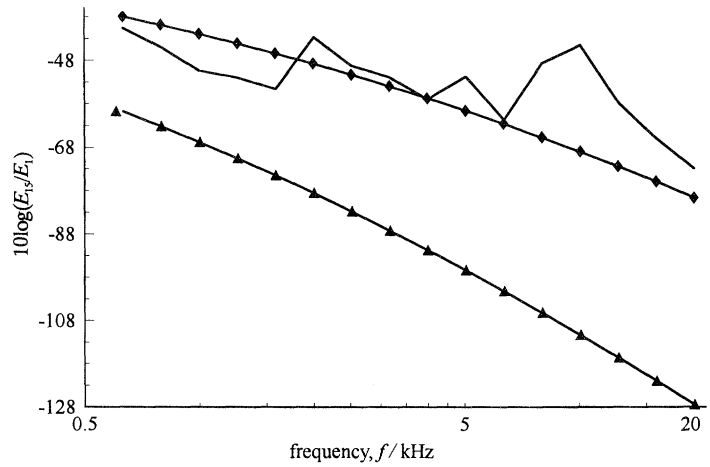

Figure 4. Bending energy in the last plate of the fifteen plate structure with simple support coupling rather than direct connections. Unmarked curve: exact results. Diamond symbols: WIA results. Triangle symbols: SEA results.

is not considered by SEA: waves that are near normal to the various junctions tend to have a high transmission coefficient in comparison with other wave headings, and thus the wavefield becomes less and less diffuse as the vibration travels down the structure. Results for the bending vibrational energy of the final plate over the full frequency range are shown in figure 3, where the under prediction arising from SEA is again apparent. For comparison, results for 'bending only' transmission are shown in figure 4; in this case the structure is taken to be 'flat' with line simple support connections, so that no in-plane waves are generated. The differences between figures 3 and 4 are due solely to the effects of in-plane waves. As might be expected the presence of in-plane waves increases the bending vibrational energy of the structure, as the in-plane dynamics provides an additional 'flanking path' for vibration transmission.

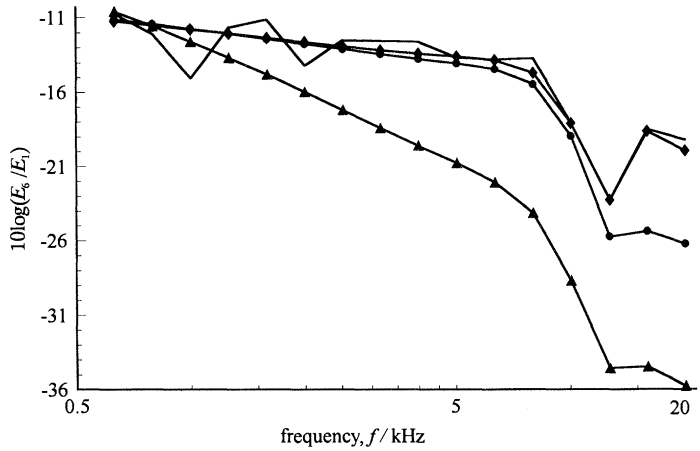

Figure 5. Bending energy in the last plate of the stiffened plate array. Unmarked curve: exact results. Diamond symbols: WIA results for a high number of Fourier terms. Circle symbols: WIA results for a low number of Fourier terms. Triangle symbols: SEA results.

The second example structure consists of a flat row of six plates which are coupled via stiffeners. Each plate has width 0.5 m and thickness 2 mm while the plate lengths (in metres) are 0.3, 0.26, 0.33, 0.28, 0.24 and 0.36. In this case the structure is considered to be made from aluminium which has Young's modulus $E = 7.3 \times 10^{10}$ N m^{-2}, mass density $\rho = 2800$ kg m^{-3}, and Poisson ratio $\nu = 0.33$. The plates are coupled through *symmetrically arranged* rectangular stiffeners of thickness 3 mm and height 200 mm. As in the previous example, the first plate is subjected to an out-of-plane harmonic point load and the dynamic stiffness method has been used to compute the third octave band energy levels. For this example the symmetric arrangement of the stringers prevents the generation of in-plane waves; in this case the aim was to investigate the role of the elastic coupling without the complicating effects of the in-plane dynamics. The vibrational energy in the final plate is shown in figure 5, where it can be seen that SEA again leads to a severe under prediction of the response. Two curves are shown for WIA; one corresponds to the use of five Fourier terms in the inner plate and three Fourier terms in the two outmost plates, while the other corresponds to the use of 41 and 20 Fourier terms respectively. It can be seen that the use of relatively few terms is adequate until around 10 kHz, beyond which the additional terms are needed to capture the behaviour of the exact results. The dip in the response curve at around 15 kHz is related to the behaviour of the wave transmission coefficient of the junction; it should be noted that simple beam theory has been used to model the stiffeners, so that internal dynamic effects have not been considered. The angular dependency of the wavefield in the final plate at 20 kHz is shown in figure 6. Here θ is defined such that $\theta = 0$ represents a wave which is normal to the junction line. The exact curve which is shown in this figure has been deduced from the dynamic stiffness analysis; with this approach the lateral dependency of the response is modelled by a Fourier sine series. As the wavelength of the bending waves at any particular frequency is known, it is possible to compute the heading of the waves whose projected wavelength corresponds to a particular Fourier sine component. A plot of vibrational energy against Fourier sine component may thus be converted to a plot of vibrational energy against wave heading. It is clear from figure 6 that the wavefield is far from diffuse, and good agreement between

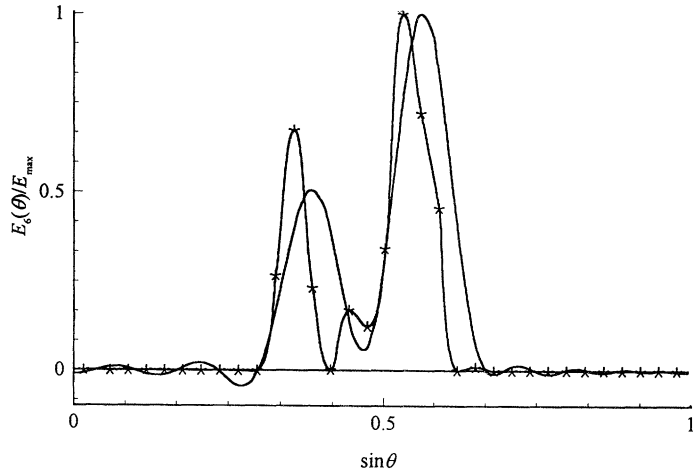

Figure 6. Bending energy variation with wave heading for the final plate of the stiffened plate array. One-third octave band with centre frequency 20 kHz. Unmarked curve: WIA results. Star symbols: exact results.

the exact and WIA results is found. The small region of negative energy that is predicted by WIA may be corrected by the addition of further Fourier terms.

Further examples which cover a wide range of structures have been presented by Bercin (1993).

5. Conclusions

The wave intensity technique which has been presented here is a natural extension of conventional SEA. It has been shown that the method can yield much improved response predictions over SEA with relatively little additional computational effort. It has further been demonstrated that the method can be cast into the form of conventional SEA with the addition of non-direct coupling loss factors, which provides a link with earlier work and with other enhancements of SEA. Although only plate structures have been considered here, the method is applicable to the same wide range of structures as SEA.

References

Bercin, A. N. 1993 High frequency vibration analysis of plate structures. Ph.D. thesis, Cranfield Institute of Technology, U.K.

Blakemore, M., Jeffries, B., Myers, R. J. M. & Woodhouse, J. 1990 Exploring statistical energy analysis on a cylindrical structure. *Proc. Inst. Acoust.* **12**, 587–593.

Cremer, L., Heckl, M. & Ungar, E. E. 1988 *Structure-borne sound*, 2nd edn. Berlin: Springer-Verlag.

Dowell, E. H. & Kubota, Y. 1985 Asymptotic modal analysis and statistical energy analysis of dynamical systems. *J. appl. Mech.* **52**, 949–957.

Kubota, Y. & Dowell, E. H. 1986 Experimental investigation of asymptotic modal analysis for a rectangular plate. *J. Sound Vib.* **106**, 203–216.

Langley, R. S. 1989*a* Application of the dynamic stiffness method to the free and forced vibrations of aircraft panels. *J. Sound Vib.* **135**, 319–331.

Langley, R. S. 1989*b* A general derivation of the statistical energy analysis equations for coupled dynamic systems. *J. Sound Vib.* **135**, 499–508.

Langley, R. S. 1990 A derivation of the coupling loss factors used in statistical energy analysis. *J. Sound Vib.* **141**, 207–219.

Langley, R. S. 1992 A wave intensity technique for the analysis of high frequency vibrations. *J. Sound Vib.* **159**, 483–502.

Langley, R. S. & Heron, K. H. 1990 Elastic wave transmission through plate/beam junctions. *J. Sound Vib.* **143**, 241–253.

Lyon, R. H. 1975 *Statistical energy analysis of dynamical systems: theory and applications.* Cambridge, Massachusetts: MIT Press.

Zienkiewicz, O. C. 1977 *The finite element method.* London: McGraw-Hill.

PHILOSOPHICAL TRANSACTIONS OF THE ROYAL SOCIETY A MATHEMATICAL, PHYSICAL & ENGINEERING SCIENCES